GEODYNAMICS & TECTONOPHYSICS
Published by the Institute of the Earth's Crust, Siberian Branch, Russian Academy of Sciences

TECTONOPHYSICS

2023 VOLUME 14 ISSUE 2 ARTICLE 0690

ISSN 2078-502X

DOI: 10.5800/GT-2023-14-2-0690

INFLUENCE OF THE EVAPORITE FORMATION STRUCTURE ON SALT TECTONICS AND HYDROCARBON TRAPS (BY THE RESULTS OF NUMERICAL SIMULATION OF HALOKINESIS IN THE PRE-CASPIAN)

B.V. Lunev [1], **V.V. Lapkovsky** [1]✉, **M.P. Antipov** [2], **Y.A. Volozh** [2], **I.S. Postnikova** [2]

[1] Trofimuk Institute of Petroleum Geology and Geophysics, Siberian Branch of the Russian Academy of Sciences, 3 Academician Koptyug Ave, Novosibirsk 630090, Russia

[2] Geological Institute, Russian Academy of Sciences, 7-1 Pyzhevsky Ln, Moscow 119017, Russia

ABSTRACT. Within the Pre-Caspian sedimentary basin, there is certain regularity in the distribution of types of structures of salt tectonics. It is characterized by concentric zoning corresponding to the change in the sedimentation thickness of the evaporite sequence. As it increases from 0 to 6 km towards the center of the basin, stamp (embryonic) salt uplifts are replaced by salt pillows first and then by salt domes and diapirs, finally changing to salt massifs and amoeboid-shaped salt ridges. In addition, diapirs in the sections of the Pre-Caspian basin, drawn from the drilling and seismic data, are shaped like high-amplitude "fingers" with a flat base, which is not a typical picture of the Rayleigh – Taylor instability development. Since halokinesis is the main factor controlling the migration and accumulation of hydrocarbons in the Pre-Caspian region, background and aim of prospecting and exploration require identifying the specifics of the formation of various types of salt structures and the relationship between their location patterns and halokinesis process.

Numerical simulation shows that, depending on the instable layer thickness and its relationship with the total thickness of the overlying layers, the instability development occurs at different rates, forming different types of structures. When the thickness of the instable layer is greater than or comparable to the thickness of the denser overburden, there occur the salt masses. A greater thickness of the overlying layer gives rise to the formation of classical mushroom-shaped diapirs. A small-thickness low-density layer first undergoes a full bending as it rises, so that its top and bottom turn out to be morphologically similar to each other, thus giving a misleading impression of ordinary stamp folds. Somewhat greater thickness of the low-density layer leads to the development of "pillows" therein. Detailed modeling made it possible to relate the specific shape of the Pre-Caspian diapirs to the fact that the basal and top horizons of the evaporite formation, being composed mainly of terrigenous, carbonate and sulfate rocks, have a normal, non-inverse density and mask complex diapiric structures of halite-saturated domal cores.

KEYWORDS: salt tectonics, halokinesis; numerical modeling; Pre-Caspian region; oil and gas potential

FUNDING: The research is a part of the state assignment of the IPGG SB RAS (project FWZZ-2022-0009) and the GIN RAS.

RESEARCH ARTICLE

Correspondence: Vladimir V. Lapkovsky, lapkovskiivv@ipgg.sbras.ru

Received: June 9, 2022
Revised: October 20, 2022
Accepted: November 11, 2022

FOR CITATION: Lunev B.V., Lapkovsky V.V., Antipov M.P., Volozh Y.A., Postnikova I.S., 2023. Influence of the Evaporite Formation Structure on Salt Tectonics and Hydrocarbon Traps (by the Results of Numerical Simulation of Halokinesis in the Pre-Caspian). Geodynamics & Tectonophysics 14 (2), 0690. doi:10.5800/GT-2023-14-2-0690

© Lunev B. V., Lapkovsky V. V., Antipov M. P., Volozh Y. A., Postnikova I. S., 2023

1. INTRODUCTION

Halokinesis is the main factor in the formation of the Pre-Caspian structures and, therefore, the main controlling factor for hydrocarbon migration and accumulation [Volozh et al., 2003]. As formulated in [Antipov, Volozh, 2012, p. 48], background and aim of prospecting and exploration require "identifying regional specific features of the structure of salt-bearing and supra-salt complexes on one hand and relating location patterns of different-type salt structures to halokinesis on the other". In the publication cited, this problem was solved based on generalization of the results of the studies made in the last two decades [Bakirov et al., 1992; Volozh et al., 1989, 1997a, 1997b, 2000; Eskozha et al., 2007; Kuandykov et al., 2011; Matusevich, 2005, 2007; Pisarenko et al., 2011]. There were performed structural mapping of the top of the salt in the Pre-Caspian basin with the use of the research results obtained by A.V. Matusevich, L.F. Volchegursky, M.S. Trokhimenko and others, sediment thickness mapping of the Permian halogen formation, and bathymetric mapping of the Permian salt-bearing basin of the Pre-Caspian region [Volozh et al., 1997a, 1997b, 2003; Eskozha et al., 2007; Matusevich, 2005, 2007]. There was determined the stratigraphic range of the Permian halogen formation (Upper Artinskian – Kazanian); besides, a stratigraphic section was drawn for the division of the Upper Artinskian – Kungurian interval of the salt-bearing unit, and stratigraphic division was carried out for the supra-salt complex of the Pre-Caspian basin [Volozh et al., 2000; Pisarenko et al., 2011; Tikhvinsky, 1974; Yatskevich et al., 1990]. Finally, in [Antipov, Volozh, 2012], there was developed the principal model for the formation of the salt-bearing unit within the Permian basin of the Pre-Caspian region. There was carried out typification for the salt structures, and a new version of zoning the salt-bearing and supra-salt complexes was proposed based on the section and structure types. In order to relate the location patterns of different-type salt structures to halokineses, consideration was given to possible scenarios of the development of salt tectonics. However, this involved the qualitative analysis of the structures identified as a result of the geological and geophysical studies. In the present paper an attempt is made to specify these relationships, the halokinetic process, and the features of halokinetic structures by numerical modeling of this process as applied to the conditions of the Pre-Caspian salt basin.

2. CHARACTERISTICS OF THE RESEARCH OBJECT

The halogen formation of the Pre-Caspian basin covers an age range from the Upper Artinskian of the Lower Permian to the Upper Kazanian of the Upper Permian. In accordance with composition and structural features, this formation is divided into three complexes: Upper Artinskian – Kungurian, primarily halogen (consists of 95 % rock salt), Ufimian terrigenous-halogen and Kazanian terrigenous-carbonate-halogen, wherein the salt interlayers (up to 30 %) are of subordinate importance. Based on the calculations made with regard to the recent geophysical data [Antipov, Volozh, 2012], the so called sediment thickness of the halogen formation is as great as 4500 m. Of this, 2500–3000 m is accounted for by the Upper Artinskian – Kungurian complex, and 1000–1500 m – by the Ufimian and Kazanian. In the Pre-Caspian salt basin margin, the lower and the upper complexes of the halogen formation are separated by a 150–610 m thick Lower Kazanian intersalt unit composed of terrigenous deposits (Sosnovskaya formation) in the east and sulfate-terrigenous-carbonate deposits (Kalinovskaya formation) in the west.

Based on the analysis of seismic and drilling data, there were determined the paleodepths of the Kungurian and Kazanian salt accumulations, and there were performed bathymetric mapping for the pre-Kungurian salt basin and sediment thickness mapping for the Permian halogen formation as a whole (Fig. 1) [Antipov, Volozh, 2012].

The principal structure of the evaporite formation is shown in Fig. 2.

The structure of the Permian halogen formation has the following features [Antipov, Volozh, 2012].

1. Sharp differences in sediment thickness of the halogen formation in the central and marginal parts of the Pre-Caspian basin – the sediment thickness of salt-bearing formation in the central part of the basin is three times greater than that on the stepped slopes. This increase is primarily due to a twofold increase in thickness of the predominantly halogen Upper Artinskian – Kungurian complex.

2. Considerable differences in the lithological composition of the sections of the Upper Artinskian – Kungurian salt-bearing complex in the northwestern and southeastern margins of the Pre-Caspian basin. In the northeast, there are three lithological-facial units: carbonate-sulfate, carbonate-sulfate-halogen, and halogen. In the southeast margin, the complex also has a three-membered structure but is comprised of differently composed units: lower sulfate-terrigenous, middle halogen, and upper sulfate-terrigenous.

3. One-type character of the structure of cyclic stratigraphic subdivisions of predominantly salt-bearing Upper Artinskian – Kungurian complex in the northwestern margin – three-membered (clay – anhydrite – salt) for the salt-bearing Kungurian formation and two-membered (carbonate – anhydrite) for the Karpinsky formation in the seismic complex basement [Pisarenko et al., 2011, 2021a, 2021b]. Transgressive contact between the Permian halogen formation and underlying deposits in the marginal (originally shallow-water) zones of the sedimentary basin changing to concordant in the deep-water basin.

4. The most ancient-known salt-bearing formation – Volgogradsky – bordering with accumulative (sedimentary) shelf scarps which separated the shallow-water part of the pre-Kungurian basin from its comparatively deep zone: stepped slopes and deep-water basin.

5. A thick terrigenous salt-bearing red-color unit (similar in age to the Ufimian terrigenous-halogen and Kazanian terrigenous-carbonate-halogen complexes) occurring in the upper section of the Permian halogen formation in the central Pre-Caspian basin.

Many researchers have noted the differences in the structure of salt domes in those or other areas of the Pre-Caspian

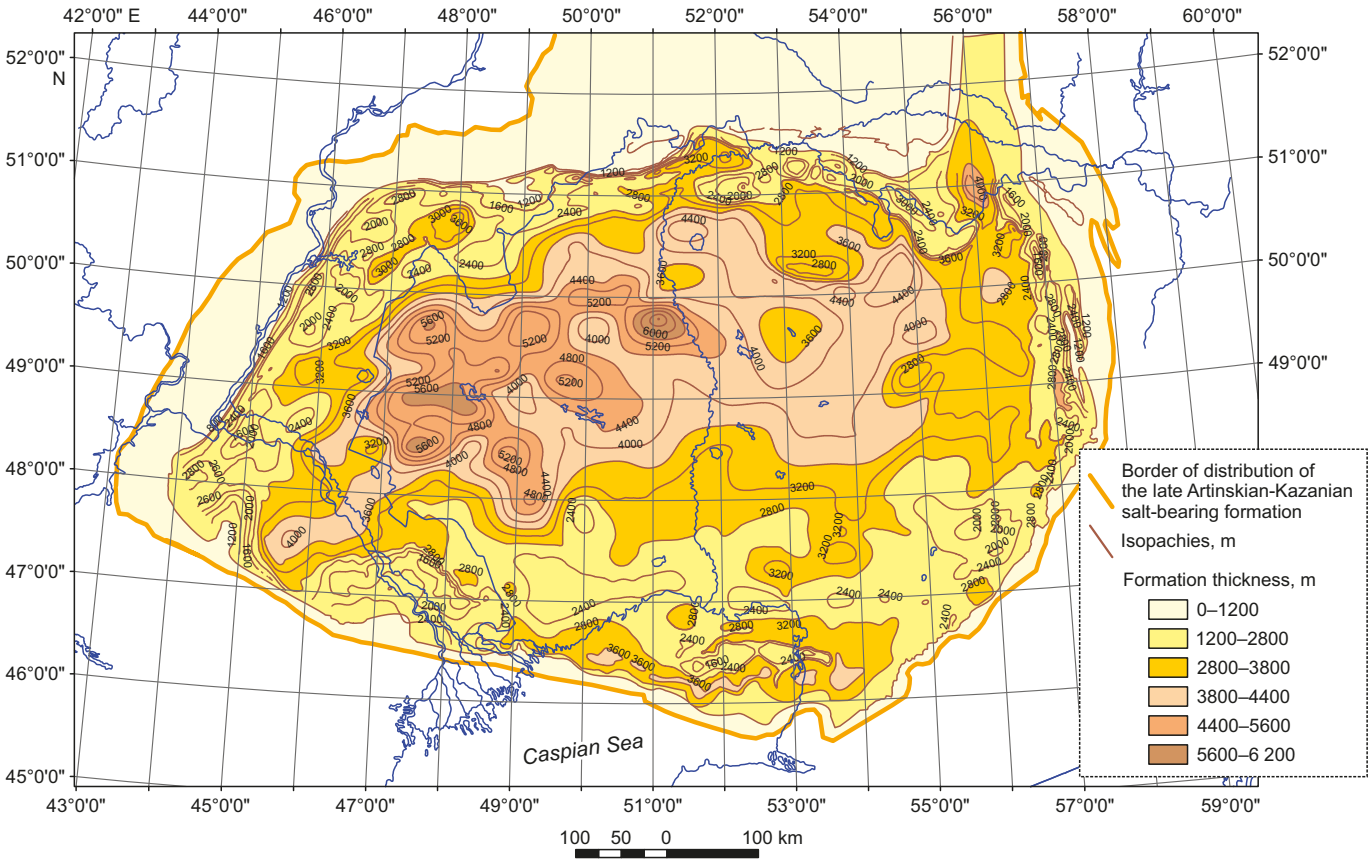

Fig. 1. Map of the sedimentation thickness of the halogen formation of the Pre-Caspian salt basin (after [Antipov, Volozh, 2012]).

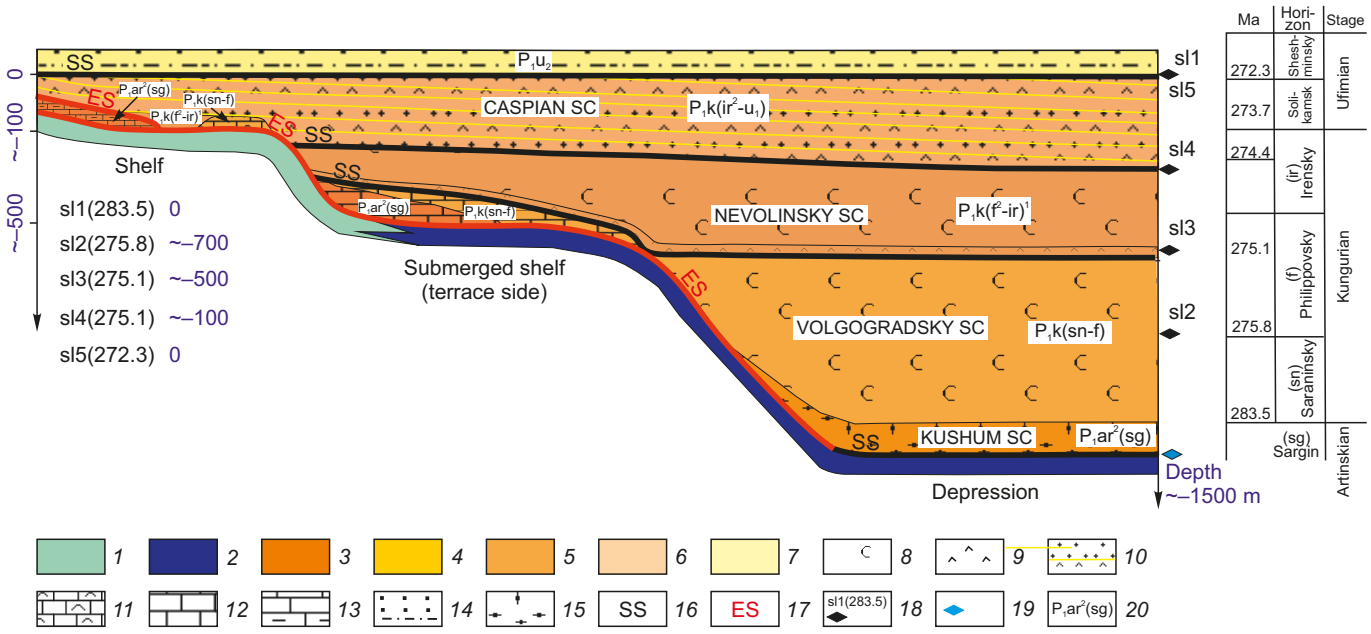

Fig. 2. Chronostratigraphic scheme of the division of the Permian halogen formation of the Pre-Caspian basin.
The scheme showing the sedimentation nature of the distribution of the evaporite formation within the Kungurian basin and its temporal paleodepth variation from 1500 m before the formation accumulation to its completion at the end of the Ufimian, with less than 50 m deep isolated continental water bodies. The process of development of the salt basin exhibits several different sea-level stages. The time for each stage was calculated conventionally based on the rate of salt accumulation in the evaporite basins.
1 – shallow water deposits of the subsalt complex; *2* – deep-water formations of the subsalt complex; *3–7* – seismic complexes (SC) of the evaporite formation: *3* – Kushum Upper Artinskian (Sargin) SC, *4* – Volgogradsky-Saraninsky-Philippovsky SC, *5* – Nevolinsky Filippovsky-Irensky SC, *6* – Caspian Irensky-Ufimian SC, *7* – Upper Ufimian terrigenous SC; *8* – halites; *9* – anhydrites; *10* – rhythmic salt-bearing strata with potassium salts; *11* – sulfate carbonates with possible content of reefs; *12* – limestones and clastic carbonate

deposits, the products of reef and carbonate platform degradation (reef and platform basement deposits); *13* – terrigenous-carbonate deposits; *14* – terrigenous deposits; *15* – deposits of underwater fans within the basin; *16* – sedimentation surface; *17* – erosion surface; *18* – sea level marks for different stages of the evaporite basin development, in brackets is the time interval in million years; *19* – mark of the depth of the Kungurian basin; *20* – stratigraphic indices of seismic complexes.

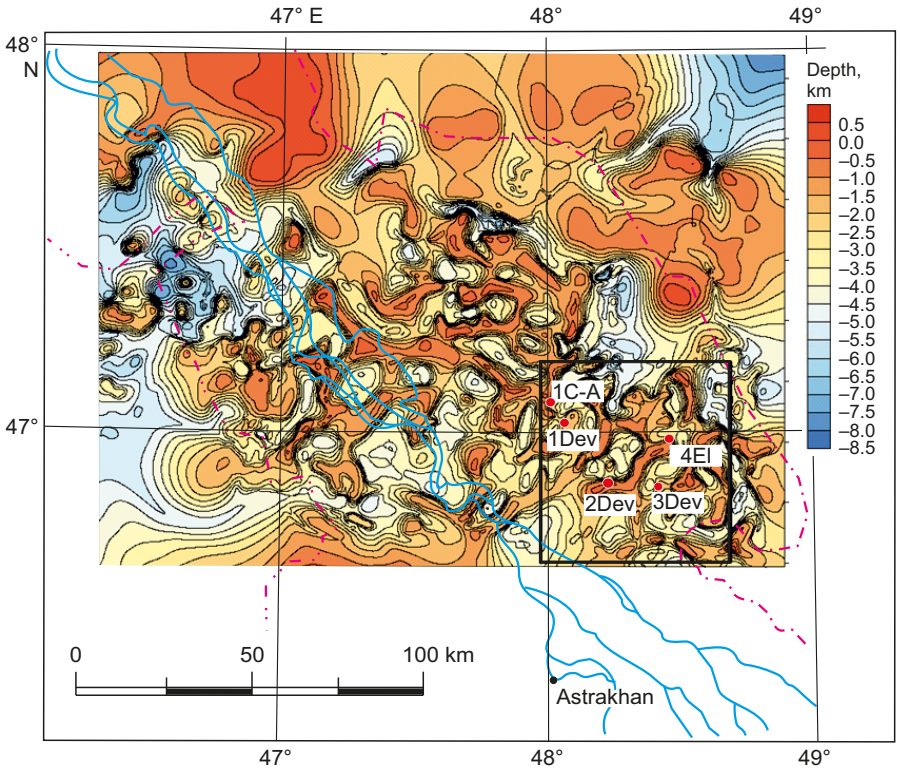

Fig. 3. A fragment of the structural map of the top of the Permian salt deposits in the southwestern Pre-Caspian after [Antipov, Volozh, 2012]. The 3D modeling area is marked with a black rectangle. 1Dev, 2Dev, 3Dev – 1st, 2nd and 3rd Devonian wells, 1C-A – Astrakhanskaya well.

basin and drawn zoning schemes for this basin based on the types of these domes [Volozh, 1971; Volozh et al., 1989, 1997b, 2000, 2003; Eskozha et al., 2007; Zholtaev, 1966; Zhuravlev, 1963, 1964, 1966; Konishchev, 1982; Volozh, Konishchev, 1989; Konishchev et al., 1990; Kosygin, 1950, 1960]. In [Antipov, Volozh, 2012], based on the newly obtained information, there are proposed a map of the top of the Permian salt-bearing strata in the Northern Pre-Caspian (Fig. 3) and a new zoning scheme for the Permian salt in the Pre-Caspian basin (Fig. 4).

Based on the structural features of the Permian halogen formation, within the Permian salt in the Pre-Caspian basin there are distinguished the Pre-Caspian salt-dome province and the Northwestern peripheral area. Inside the Pre-Caspian salt-dome province, there are distinguished eight seismogeological areas: Northern, Western, Southern, Southeastern, Central Pre-Caspian, North Caspian – Aktobe, Karasal–Smushkov, and Primugodzhar (Fig. 4).

Within the identified areas, there are observed the following location patterns of the salt structures of different types.

Stamp (embryonic) salt uplifts are located along the northwestern peripheral area, in the zone bounded by the Paleozoic carbonate platform's scarp from the inside and by the line of current distribution of the salt-bearing strata from the outside. The thickness of the salt-bearing complex therein varies from 0 to 1200 m, that of the supra-salt complex – from 500 to 1500 m.

Salt anticlines are widespread in the southwestern peripheral area, in up to 10 km wide strip adjacent to the northern slope of the Karpinsky Ridge.

Toward the center of the salt basin, salt anticlines and pillows change to salt-dome development zone. It occupies the southeastern part of the basin and consists of three subzones. There is also an isolated salt-pillow zone within the Sol-Iletsk protrusion and Karasal monocline. Closer to the periphery, there are conical salt-dome structures, first changing to stepped dome and then to mushroom-shaped dome zone. The central part of the Pre-Caspian salt basin is occupied by the area of development of salt massifs and amoeboid-shaped salt ridges. And, finally, there is a narrow strip of salt bars extending along the northwestern margin of the basin. All known diapiric structures of the Pre-Caspian basin are located within its central areas.

Therefore, the location pattern of halokinetic structures has a clearly defined concentric zonality corresponding to the change in the evaporite sediment thickness.

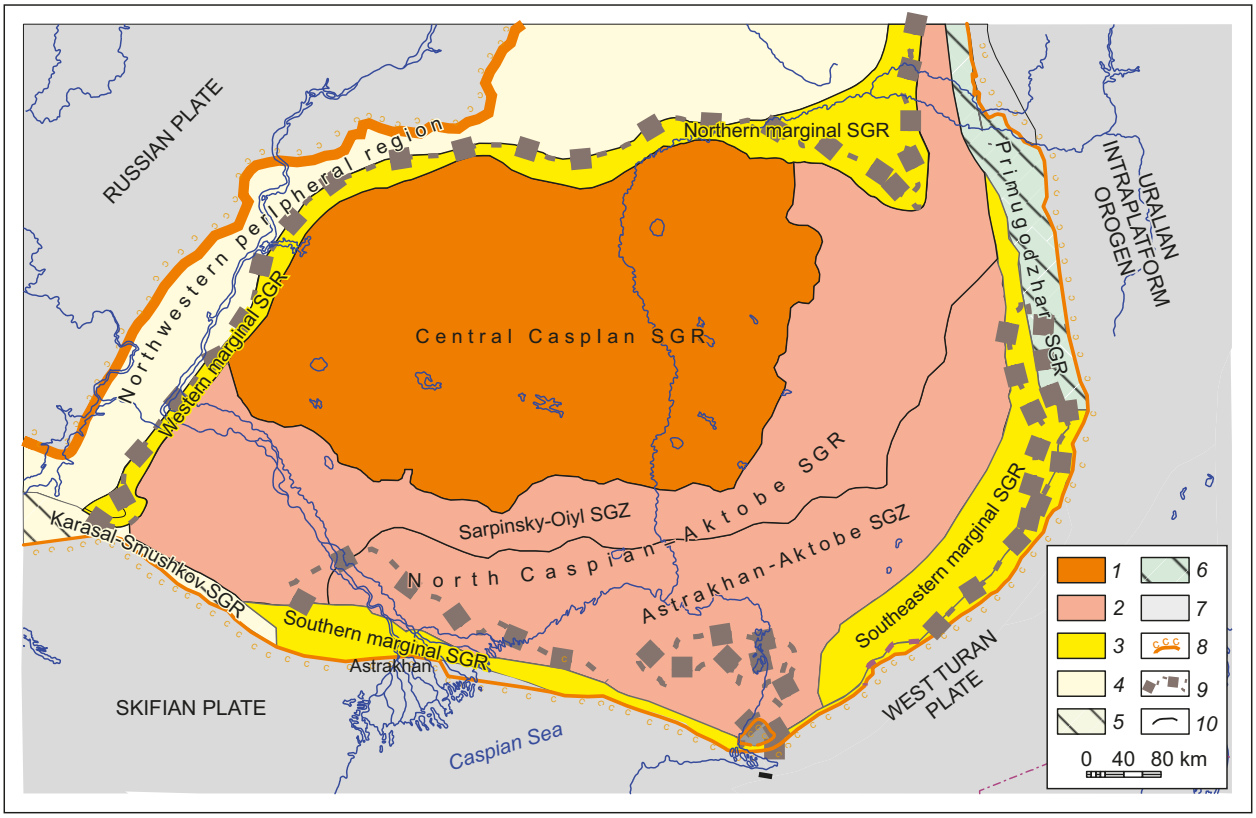

Fig. 4. Scheme of zoning of the salt and supra-salt complexes of the Pre-Caspian salt-bearing basin according to the types of sections and structures (modified from [Antipov, Volozh, 2012]).
1 – Central Pre-Caspian seismogeological region (SGR); *2* – North Caspian – Aktobe SGS, consisting of two seismogeological zones (SGZ): Sarpa-Uil and Astrakhan-Aktobe; *3* – marginal SCS: Western, Northern, Southern and Southeastern; *4* – Northwestern peripheral SGR; *5–6* – areas of development of salt anticlines (salt tectonics): *5* – Karasal-Smushkov, *6* – Primugodzhar; *7* – area of no Kungurian salt-bearing deposits; *8* – the boundary of the distribution of the saline Upper Artinskian-Kazanian formation of the Pre-Caspian salt basin; *9* – boundary between the Bashkirian intra-basin carbonate platforms and the Permian carbonate scarp; *10* – boundary between the Sarpin-Uil and Astrakhan-Aktyubinsk seismogeological zones.

3. METHODOLOGY AND RESULTS OF MODELING

Proper formulation of the problem of creating models for halokinetic development by calculation of creeping flow in a non-uniform-density viscous liquid, its justification and solving methods are described in detail in our previous publications [Lunev, Lapkovsky, 2009, 2014; Lunev et al., 2017a, 2017b; Abramov et al., 2016; Kontorovich et al., 2014, 2019; Abramov, Lunev, 2014; Abramov, 2015]. Here we will focus only on the description of certain application of the method of generating a model of the object of study.

In order to identify key features of the development of instability of a low-density salt-saturated layer depending on its thickness in relation to the total thickness of overlying denser layers, it is worthwhile to apply our previous 2D-modeling program "Diapir" [Lunev, Lapkovsky, 2009; Filippov et al., 2009]. Its application assigns immediately the entire section showing the layers of different density and configuration and initiates an action of gravity force and a study of the system evolution.

Fig. 5 displays the development of instability of a low-density layer which varies in thickness from a few hundred to a few thousand meters.

It is evident that depending on the instable layer thickness and its relationship with the total thickness of the overlying layers, the instability develops at different rates forming different-type structures.

When an instable layer thickness is greater than or comparable to the thickness of the overlying denser rocks, the floating of the layered material gives rise to the formation of salt massifs. Such version of the instability development is confined to the right flank of the structure shown in Fig. 5. It is calculated and displayed separately in Fig. 6.

At a greater thickness of the overlying layer, there occur classic mushroom-shaped diapirs as seen in the middle part of the structure in Fig. 5 and separately in Fig. 7.

And, finally, a thin low-density layer, when floating, first bends completely over so that the morphology of its top is similar to the morphology of its bottom, thus creating a false impression of typical stamp folds (Fig. 8). Some increase in the low-density layer thickness leads to the development of "pillows".

In Fig. 5, the development of the pseudo-stamp folds takes place in the left flank of the structure. Between these folds and the diapir formation zone, there is observed the development of "pillows".

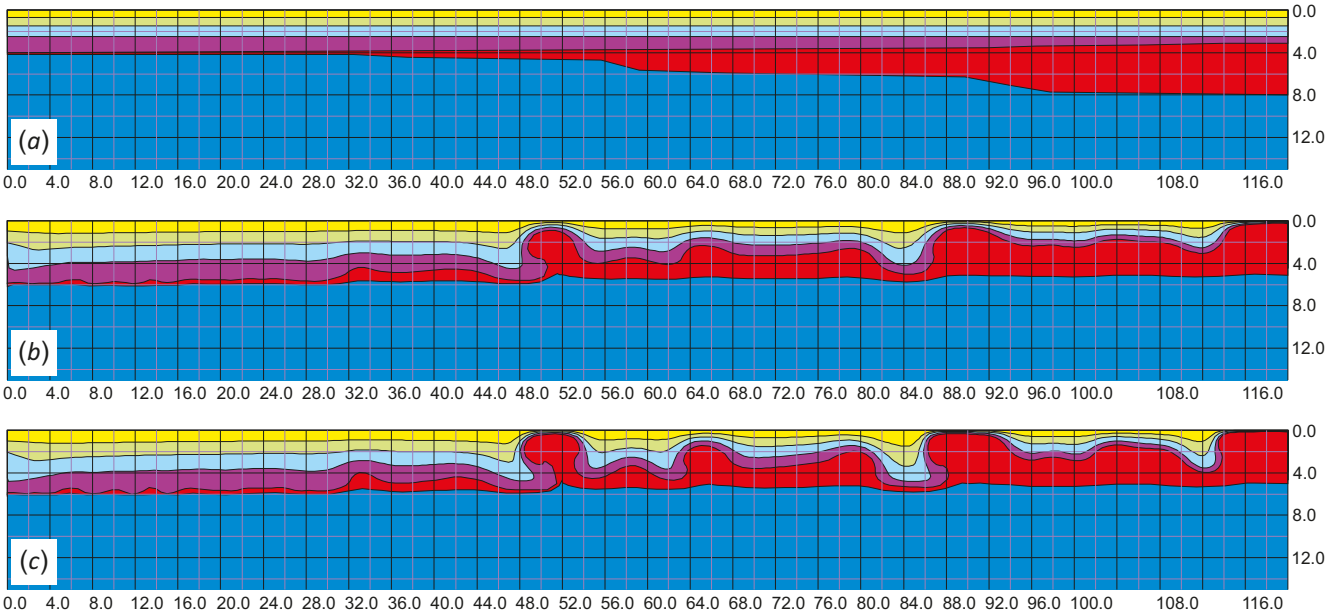

Fig. 5. Stages of development of instability of a low-density variable-thickness layer.
(*a*) – initial stage, (*b*) – intermediate stage, (*c*) – last calculated stage. The instable (low-density) layer is shown in red, the overlying denser layers are shown in other colors, and the underlying, densest layers are shown in blue. (A thin red layer on the left flank is almost invisible due to image scaling). Horizontal scale (bottom) and vertical scale (right) dimensions here and below are shown in km.

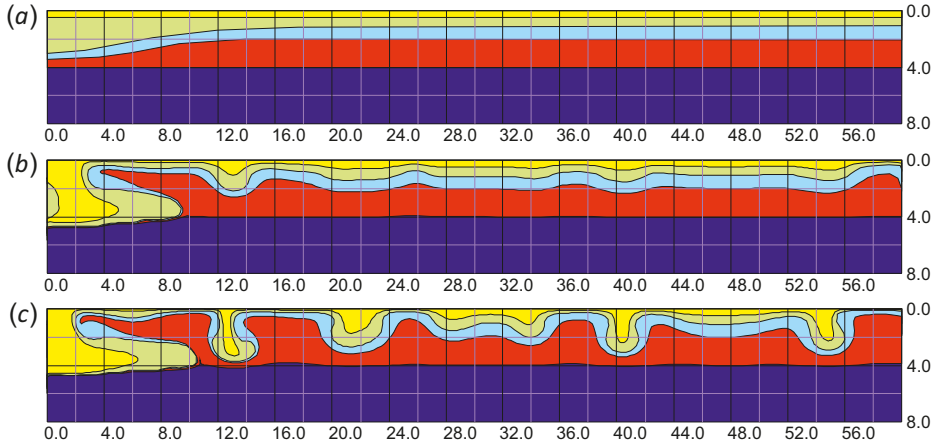

Fig. 6. Development of instability of a thick low-density layer (red) overlain by a denser sequence of layers of the same thickness.

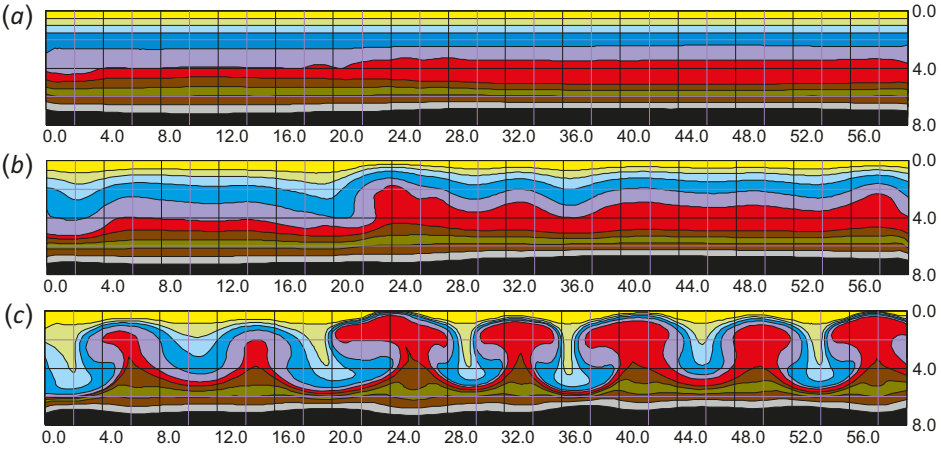

Fig. 7. Development of instability of a low-density layer (red), whose thickness is about half as much as that of the overlying denser sequence of layers – the growth of mushroom-shaped diapirs.

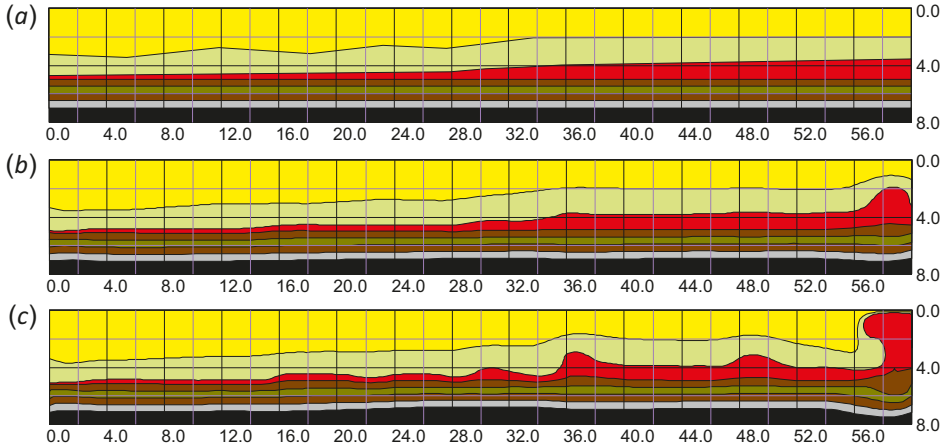

Fig. 8. The development of instability of a thin low-density layer (red) with the formation of pseudo-stamp folds, which change to "pillows" with the increase in the instable layer thickness on the right side.

A different character of the instability development structures is due to the interaction between two main factors. First, a typical horizontal dimension of emerging structures (the evolving instability wavelength) is determined by the convective layer thickness from the bottom of the floating low-density layer to the depth where its density is greater than that of the overlying material, in this case – to the free surface. Second, the thicker the inversion layer (at a given value of the density deficit), the faster the instability development because the larger the anomalous masses, the larger the buoyant force and, respectively, the faster buoyancy-induced flow rates. Therefore, in the thicker floating layer zone the intensifying disturbances have an opportunity to float to the surface and create clearly defined diapirs whereas in the zone of a thin instable layer its bending amplitude remains relatively small. The development of salt massifs in the zone where the floating layer thickness is greater than or comparable to the total thickness of the overlying layers can be attributed to mere lack of space for the mushroom-shaped diapir formation.

The results of modeling are consistent with the above description of the zonal location of halokinetic structures (see Fig. 4) and with the change in thickness of the halogen formation sediment in the Pre-Caspian salt basin (see Fig. 1), thus providing a sufficient explanation thereof. This eliminates the need to suggest that the external forces may result in the formation of salt stamp folds in the peripheral zone of salt-bearing deposits with the initially small thickness. This possibility cannot be ruled out, but it contradicts the observed structure of the top of the Caspian evaporite formation (see Fig. 3) which corresponds to the classical pattern of development of the Rayleigh – Taylor instability with a sustained characteristic wavelength of perturbations. In relation to this, it may also be noted that the above-mentioned formation of the system of bars subparallel to the salt-bearing area margin is obviously based on the marginal effect which follows directly from the salt basin geometry.

A more detailed analysis of the influence of the section structure on halokinesis and character of the resulting structure involved the use of "Diapir3D" program [Abramov et al., 2018]. This program allows making calculations in accordance with the existing 3D dimensions of the observed structures (see Fig. 3); besides, it provides a possibility to calculate the Raleigh-Taylor instability development against the background of the assigned section formation – vertical motions accompanied by the accumulation and irreversible consolidation of sediments at the subsidence of the area and by their erosion at the uplift.

For modeling, there was chosen the location (see Fig. 3) within the North Caspian – Aktobe region corresponding to the subsided shelf of the pre-Kungurian sea basin (see Fig. 2). There was an attempt to reproduce the currently observed modern structure of the evaporite formation as nearly as possible. No consideration has yet been given to achieving close similarity between the model and the object studied; we only tried to reproduce the reliably identified features of the structure – its general configuration (on-site location of domes and interdome synclines) and hypsometric marks of the evaporite formation on the tops of the domes and in the depressions in accordance with the mapped surface (see Fig. 3), and a general hypsometric position of its bottom in accordance with the drilling data [Volozh, Parasyna, 2008]. In relation to this, we have not yet used the available possibility to assign changes to the on-site regional background motions and deposit compositions. It was supposed that regional vertical motions at every moment of time were uniform throughout the location and that the deposit composition (expressed as the deposit density), averaged across the distinguished layers, is also uniform over the entire location.

The subsidence rates in this area were calculated as constants for each distinguished layer based on its thickness and geological age of its boundaries, with regard to the desired law of sediment consolidation. The uplift rates were calculated based on various assumptions about the total amount of erosion during the gap in sedimentation. (Just note that this parameter of the model, for obvious reasons, can vary in a wide range.) It was therewith supposed that the subsidence in the area is compensated by

irreversible consolidation of sediments, and the uplift – by erosion. Therefore, the average location of day surface on the studied area remains unchanged to within a certain constant, and its relief is determined by dynamics of anomalous masses arising from the development of density instabilities, i.e. by halokinesis. The density is determined as a function of the average composition assigned for each layer and the law of consolidation implying interpolation between the density values assigned for each layer at certain depths.

We calculated several tens of instability development versions which model the evolution of salt structures in the selected location at different parameters. The parameters of the final-state model, best aligned with the observation data on hypsometric marks of the top of evaporites domes and in the bottoms of interdome synclines, and average hypsometric values of their basements are presented in Table 1 (thickness of the distinguished layers and age of layer boundaries) and in Table 2 (the laws of density variation).

The model-assigned division of the evaporite formation into three layers – layers № 6–8 in Tables 1, 2 – needs explanation.

A relatively high-density layer at the top of the evaporite formation (layer № 8 in Tables 1, 2) is distinguished by the fact that the Pre-Caspian cross-sections drawn from the drilling and seismic data, presented in publications [Pisarenko et al., 2011, 2021a, 2021b], usually show diapirs in the form of large-amplitude fingers, with only a few of them mushroom-shaped corniced. It is known, however, that most of the diapirs, at the amplitudes which occur in the study area, are exactly mushroom-shaped [Jackson, Talbot, 1986]. However, the cross-sections and the map show the top of the entire evaporite formation, not the top of a certain halite-saturated instable layer. We assumed that if the upper part of the formation has a high terrigenous and high-density anhydrite or dolomite content, then, with the growth of diapirs, it will envelope them masking the mushroom shapes and making the finger-like structures. As shown by the results of modeling, this assumption proved correct. The basis for this assumption lies in the fact that the upper evaporite formation of the southwestern Pre-Caspian really includes sulfate-terrigenous and carbonate-anhydrite-terrigenous strata (see Fig. 2).

The assumption about the initial presence of a relatively high-dense, a few hundred meters thick layer in the basement of the evaporite formation (layer № 6 in the Table 1, 2) is based on the following considerations.

Though the root zones of the real salt diapirs understandably remain almost unexplored, numerous centrifuge experiments [Ramberg, 1985] show upward bending of the base of the floating layer – the material of the underlying horizons is involved in the diapir to a larger or smaller height depending on the ratio of densities and diapir maturity. As shown by our numerical experiments [Lunev, Lapkovsky, 2014], the deeper layers in this process undergo inverse folding: the synclines are formed beneath the diapirs, and the anticlines – beneath the interdome depressions. The amplitude of folding may reach a few hundred meters (at a width coinciding with a diapir wavelength) and attenuates down the section in the depth range up to 1–2 km beneath the instable layer. Degree of manifestation,

Table 1. Model parameters of the section

Layer number	Age of the top of the layer, Ma	Layer thickness, m	Stratigraphic nomenclature of the layer
1	359	0	D
2	323	790	C2t-v-s
3	315	140	C2 b
4	299	50	C2 m+C3
5	284	100	P1s-a
6	280	700	P1k
7	278	500	P1k
8	273	800	P1k+P2(?)
9	201	2700	P3+T
10	174	–1000	J1
11	145	300	J2-3
12	66	300	K
13	10	1100	KZ
14	5	–1000	KZ
15	0	300	KZ

Note. The red color in Table 1 shows the intervals where the accumulation of sediments was replaced by sediment erosion, and the model-inferred eroded thicknesses of the earlier deposits are negative. The zero value of the thickness beneath the boundary № 1 implies no borders thereunder (in the model).

Table 2. Density change dependency

Layer number	Layer thickness, m	Depth H=0	H=1000 m	H=2500 m	H=7000 m	H=9000 m
1	0	2700	2700	2700	2700	2700
2	790	2700	2700	2700	2700	2700
3	140	2600	2600	2600	2600	2600
4	50	2500	2500	2500	2500	2500
5	100	2500	2500	2500	2500	2500
6	700	2450	2450	2450	2450	2450
7	500	2200	2200	2200	2200	2200
8	800	2450	2450	2450	2450	2450
9	2700	1900	2250	2350	2500	2520
10	–1000	1900	2250	2350	2500	2520
11	300	1900	2250	2350	2500	2520
12	300	1900	2250	2350	2500	2520
13	1100	1900	2250	2350	2500	2520
14	–1000	1900	2250	2350	2500	2520
15	300	1900	2250	2350	2500	2520

Note. The first column is the number of layer (from bottom to top), the second column is the initial thickness (zero value for the first layer, as well as in Table 1, means the absence of underlying boundaries in the model), the next columns are deposit densities at specified depths for calculating the consolidation of sediments as they get buried.

amplitude and rate of attenuation of inverse folding beneath the instable layer depend on the maturity of diapirs and density of the layers in which it develops.

Judging by the amplitude of diapirs in the study area, there will be expected a distinct development of the deformations described. However, based on the drilling and seismic data, the base of the evaporite formation demonstrates relatively small deviations from the sub-horizontal bedding; there was no evidence found for its upward involvement in diapirs. If the base of the evaporites is the base of an instable, halite-saturated floating layer, then such a situation (a small amount of its deformation) is only possible at very high density of the underlying layers. However, in accordance with the available data [Volozh, Parasyna, 2008], the evaporite-underlying rock density does not exceed 2700 kg per m^3.

We have therefore assumed that the base of the instable layer is located upward, and the lower part of the evaporite formation, as well as the upper, is represented by relatively high-dense carbonate or anhydrite-containing rocks. This assumption also has real grounds – in the lower parts of the formation there are sulfate-carbonate or sulfate-terrigenous layers (see Fig. 2 in particular). It is difficult to judge the initial thickness of this basal layer of the evaporite formation due to its significant deformations during the process of halokinesis. In the model proposed, its thickness – 700 m – is chosen so that it could consider the other parameters, due to which the final vertical deformations of its base (corresponding to the base of the entire evaporite formation) would remain insignificant, in accordance with the available geological and geophysical data (i.e., in such a way that this boundary was near the level separating the zones of folding, concordant with or inverse to the diapirs).

Thus, the initial structure of the evaporite formation is assigned as three-membered: with a 500-m salt-saturated low-density instable layer underlain by 700-m and overlain by 800-m denser sulfate-carbonate or sulfate terrigenous layers. Note that such structure of the formation is consistent with the general regularities in the process of evaporite accumulation [Pisarenko et al., 2011, 2017, 2021a, 2021b].

At the end of the description of the initial model, we will focus on the way of assignment of initiating disturbances which determine the localization of rising diapirs and their-separating basin-like depressions. It is known that general parameters of the system such as viscosity and ratio between thicknesses and densities of the layers determine general characteristics of the Rayleigh – Taylor instability development – a wavelength and a rate of disturbance increase. However, a certain localization of increasing disturbances (diapirs) is caused by casual coincidence of circumstances – irregular boundaries of the layers and/or lateral variations in layer densities. It is not possible to identify real initial disturbances which have caused the currently observed salt-dome structure. However, since the disturbance, which has started to increase, is developing very steadily due to the positive relationship between density distribution and deformation rate, it does not really matter for what reason this increase started – the important thing is that it started in this place. Therefore, in order to reproduce the observed structure, we just assigned the initial

disturbances as slight undulations of the top of the instable (salt-saturated) layer, coinciding in plan with the modern structure of the evaporite formation surface, in the way it is shown in the map of the top of the salt-bearing deposits (see Fig. 3).

Medium viscosity in the model is assigned by 2.5×10^{20} Pa·s.

Fig. 9 and 10 display the results of halokinetic modeling in the specified location.

In the final structure (see Fig. 9), a certain instable salt-saturated layer (№ 7 in Tables 1, 2) forms clearly defined mushroom-shaped diapirs with an upward involvement of the material of its underlying layer № 6 – the basal evaporite layer in the model, which corresponds to general regularities of the Rayleigh – Taylor instability development. As this takes place, the top of layer № 8, the upper layer of the evaporite formation in the model, envelopes these mushroom-shaped structures, masking the "caps" of the diapirs and giving them the form of large-amplitude fingers. The base of the lower evaporite formation layer (layer № 6) is slightly bent near one hypsometric level. Therefore, in spite of the complex internal structure of diapirs, the calculated configuration of the boundaries of the evaporite formation as a whole (top and base) corresponds approximately to that in the structural map of the evaporite top and in the geological sections of the southwestern Pre-Caspian drawn from the drilling and seismic data.

The calculated evolution of the structures (see Fig. 9) is characterized by the following. The first noticeable deformations with fold amplitude of a few hundred meters on top of the instable salt-saturated layer (№ 7) of the upper evaporite formation occur after the accumulation of dense layer of sediment (№ 8) on top of the formation and beginning of the Upper Permian sediment deposition. This is followed by slow increase of deformations giving rise to the formation of "pillows" during almost 100 million years, to the end of the Lower Jurassic. The accumulation of 2.7-km layer of the Permian-Triassic sediment with subsequent erosion of its upper 1000 m might have just resulted in a considerable consolidation of terrigenous deposits of that period and a corresponding increase in the total floating-layer density deficit which may have further contributed to acceleration of growth of the domes. In the following 30 million years, the pillows begin to grow rapidly, with an amplitude reaching 2.5 km by the end of the Jurassic. In the Cretaceous, the domes grow up to a height of the free surface, and the instable layer (№ 7) begins to form mushroom-shaped diapirs whose amplitude reaches 3 km. In the Cenozoic, there is a continuation of growth of the diapirs (to 4 km) and extension of their "caps" along the surface so that there sometimes occur negative folding angles and cornices even on top of the upper, dense evaporite layer (№ 8) which envelops clearly defined mushroom-shaped structures of the internal instable layer (see Fig. 9, stage VIII; Fig. 10).

As seen in Fig. 9, from the very beginning of growth of the domes, there has been an increase in layer thickness in the inter-domes synclines and a decrease in that above the domes so that the thickness of some supra-salt deposits finally decreases to almost zero. This also relates to the upper, dense evaporite layer (№ 8) whose thickness at the last stages of the evolution increases especially on the flanks of the domes. This is partly due to the consedimentary character of the evolving structure but to a larger extent – to the redistribution of the material and its withdrawal from the tops of the domes into the inter-domes synclines. It is quite obvious from the models generated using "Diapir" program, immediately assigning an already drawn cross-section and calculating its deformations rather than modeling the sediment accumulation (see Fig. 5, 7).

The subsalt layer boundaries at the "pillow" stages of the evolution before the end of Jurassic (see Fig. 9, stages I–V) are bent in accordance with the supra-salt boundaries (at deformation attenuation with depth). The Cretaceous rapid growth of the salt structures and the rise of diapirs mark the start of development of inverse folding in the subsalt layers (in accordance with [Lunev, Lapkovsky, 2014]). It is clearly defined in this model only from the lower horizons whereas the upper horizons, for example, the evaporite base (base of layer № 6), first demonstrate the formation of the under-dome anticlines whose amplitude decreases to zero at the final stage. As this takes place, beneath the diapirs there occurs the thickening of the lower evaporite layer whose top (which is also the base of the instable, salt-saturated layer) experiences the upward involvement in rising diapirs whereas the base is subsiding.

4. DISCUSSION OF THE MODEL RESULTS

As seen in Fig. 9 (stage VIII) and Fig. 10, the final structure of the area, obtained as a result of the modeled evolution, generally correlates with the actually observed (see Fig. 3). The coincidence of the structure configuration in plan is obviously due to the considered way of assignment of initially small disturbances. However, the ability of the model-generated structure to reproduce closely the real one confirms, first, the assumption that the real structure of the studied area was formed as a result of the Rayleigh – Taylor instability development and, second, that the selected model parameters more or less correspond to the reality. This is also confirmed by an approximate correspondence of the calculated and observed hypsometric marks of the evaporite top on the tops of the domes and on the bottoms of the inter-domes synclines with general hypsometry of the evaporite formation base.

The main difference between the calculated and mapped (see Fig. 3) final structure of the evaporite top lies in steeper model-generated anticline flanks. This may be due to model inaccuracy, but it is also probable that more gentle flanks of the domes on the map are attributed to surface smoothing in result of the data interpolation. Also noteworthy are some differences in surface differentiation and in some of its depth marks on the tops of the domes. This surely indicates the model imperfection and the necessity of its further refinement.

In the calculated evolution of the structure, there can be seen some inconsistency with the previous conclusions

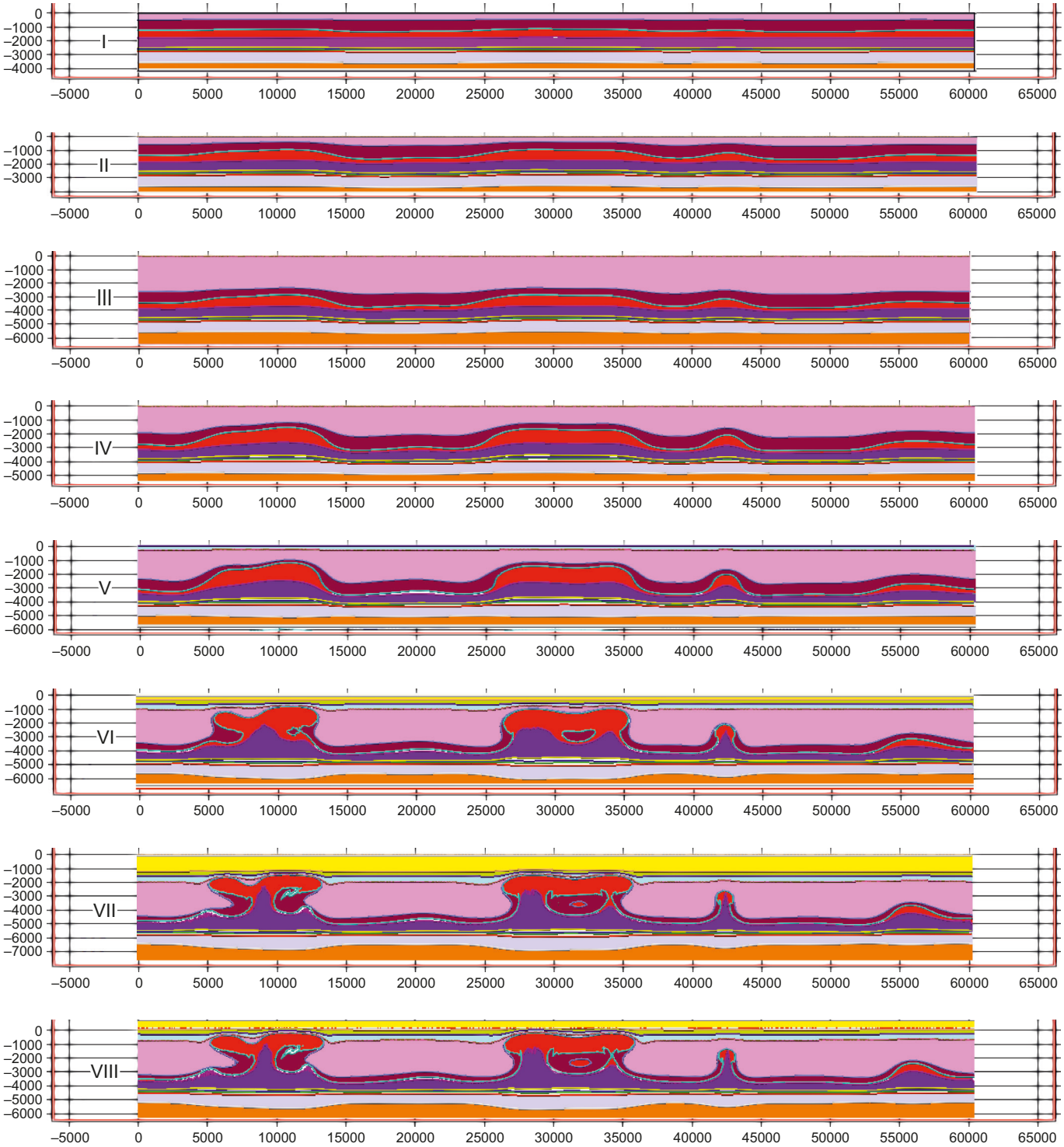

Fig. 9. Stages of the calculated evolution along the west-to-east section in the middle of the area highlighted in Fig. 1.
The upper level of the evaporite sequence is shown in red-brown, the lower – in dark lilac. The instable salt-saturated layer is shown in red therebetween.
I. About 260 Ma ago – evaporites accumulated, the Upper Permian sedimentation began – the first noticeable deformations occurred.
II. The Upper Permian continues to accumulate, with consedimentary deformations occurred therein.
III. 201 Ma ago – the 2.7-km Permian-Triassic complex has accumulated.
IV. 174 Ma ago – the 1-km Lower Jurassic erosion has completed.
V. 145 Ma ago – the accumulation of the Jurassic has completed, the "pillow" stage of the development of domes ends, and their accelerated growth starts.
VI. 66 Ma ago – the accumulation of Cretaceous deposits was completed; at that time, there occurred the main growth of domes with the formation of mature diapirs.
VII. 10 Ma ago – there was deposited the 1.1-km Paleogene and, partially, Miocene sediment layer.
VIII. 5 Ma ago, the beginning of the Pliocene epoch – there was a cut-off of the 1-km previously accumulated Cenozoic sediment.

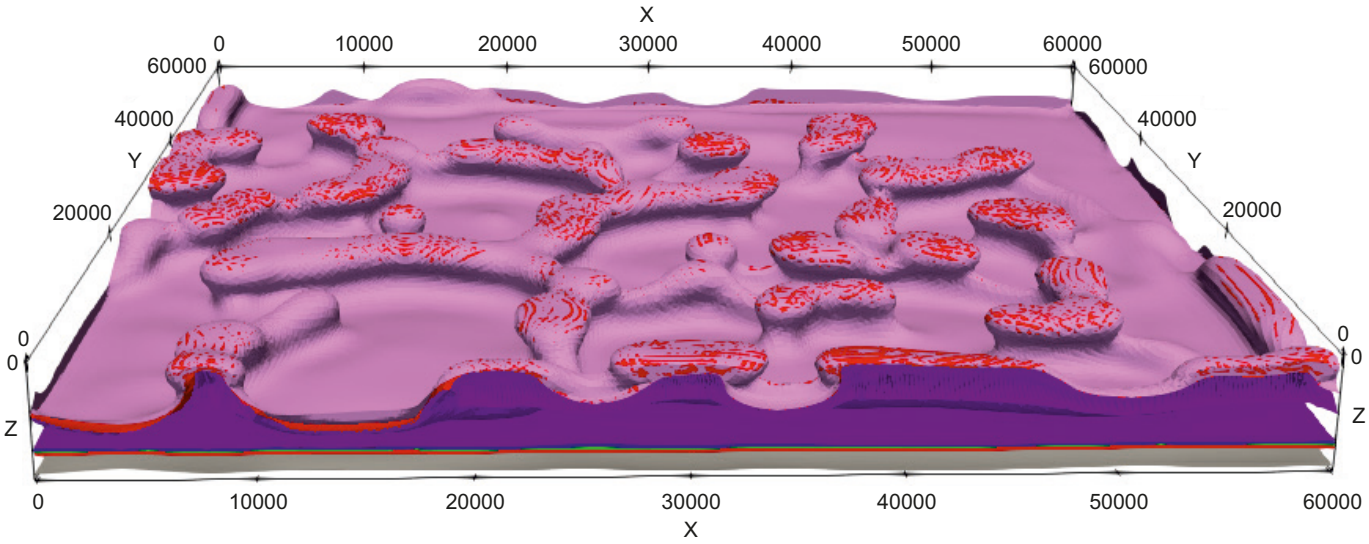

Fig. 10. Top of evaporites according to the results of modeling.

about large-amplitude halokinetic deformations occurred at the early stages, as far back as the time of the upper evaporite formation accumulation [Antipov, Volozh, 2012]. Note that according to the modeling results, the amplitude of disturbances of the instable (middle) evaporite layer top reaches a few hundred meters by the end of the upper formation accumulation (see Fig. 9, stage I). This inconsistency may be due to disadvantages of the model. For example, due to the fact that it does not consider the probability of hurricane accumulation of the upper formation, instantly smoothing the free surface. As shown in [Poliakov et al., 1993], at an instant smoothing of the free surface, the halokinetic structures are formed much faster. On the other hand, the conclusion about large-amplitude halokinetic motions at the early stages of the process, during the upper evaporite formation accumulation, was based on large variations of its present-day thickness – until disappearance on the tops of the domes – assuming that they are caused by consedimentary character of deformations. However, this is not necessarily so. As discussed above and shown by modeling (see Fig. 5, 7, 9), such variations in thickness may occur as a result of sediment redistribution of the initially invariable-thickness layer during post-sedimentary deformations. At any rate, this is the pattern of variation in the upper evaporite formation thickness provided by the model proposed.

However, the initial halokinetic stages – those of the formation of "pillows" – are usually characterized by very slow growth of disturbances [Jackson, Talbot, 1986]. Nevertheless, it makes sense for further modeling to consider the influence of high sedimentation rate as applied to the study area. Besides rapid growth of salt domes, such modeling can yield their resulting pillar-like shapes irrespective of whether or not the high-density rocks of upper evaporite formation envelope its internal structure [Poliakov et al., 1993].

In general, an approximate consistency between the model and a real structure implies that we succeeded to reproduce the principal features of halokinetic development in the southwestern Pre-Caspian and to identify the causes of their occurrence. The modeling showed a direct relationship between the lithological-stratigraphic structure of the evaporite formation on one hand and halokinesis and the character of halokinetically caused structures on the other.

The modeling allowed explaining the observed zonal location of halokinetic structures, having obviously related it to the total initial sediment thickness of the halogen formation in the Pre-Caspian salt basin. It is shown that depending on the instable layer thickness and its relationship with the total thickness of the overlying layers, the instability development occurs at a different rate forming different types of structures, just what are really observed: pseudo-stamp folding along with the increase in a relative instable-layer thickness, pillows, mushroom-like diapirs, and salt massifs. It is particular significant that this result makes it unnecessary to assume the existence of any external effects.

An assumption about the initially three-membered lithological-stratigraphic structure of the evaporite formation, with carbonate- or sulfate-filled normal (non-inverse) density layers in its base and top and the instable salt-filled low (inverse) density layer in its middle part, allowed explaining a specific character of the Pre-Caspian domes – large amplitude finger-like diapirs on the top of ervaporites whose almost smooth base is not involved high up into the diapirs. It is shown that classic mushroom-shaped diapirs, formed by the middle, instable layer, are enveloped with a higher-density material of the upper evaporite formation, which is spreading out over the domes and accumulating on the flanks so that the entire evaporite dome takes the form of a finger. As this takes place, high-density material of the lower formation causes thickening beneath the diapirs and undergoes deformations typical of the upper subsalt layers [Lunev, Lapkovsky, 2014], with its top (which is also the base of the salt-bearing, instable layer)

involved high up into the diapirs and its base (coinciding with the formation base as a whole) subsiding thereunder approximately to the initial level.

It should be said that the model thicknesses of the evaporite formation parts (700, 500 and 800 m from bottom to top) are selected more or less arbitrarily as well as their assigned densities. Identification of the actual initial lithological-stratigraphic structure of the evaporite sediment is hampered by the strongest deformations undergone during halokinesis: the upper layer on the tops of the domes is thinning until disappearance whereas the lower layer, involved in the diapirs, has subvertical bedding therein and is complexly dislocated, together with the material of the middle, instable layer. In this connection, the lithological-stratigraphic divisions based on the diapir well logging data seem questionable. This is indicated by both large-diapir well logging and seismic data showing the inability to identify the primary stratigraphic sequence within the domes because of complex rock dislocation [Pisarenko et al., 2011, 2021a, 2021b]. To solve this problem (or at least to come close to solving), it would be good to make stratigraphic division on the basis of cores obtained from a borehole drilled in the center of a large inter-domes synclines.

5. CONCLUSION

The model proposed herein is of a preliminary, estimative nature. Its generation was aimed at identifying the principal halokinetic features of the Pre-Caspian. As a result of modeling, there were determined the relationships between the features of the lithological-stratigraphic structure of the evaporite formation and the character of halokinesis, and some important questions were raised regarding its initial structure and the character of related structures.

In terms of focusing the exploration on hydrocarbons, the most interesting results of modeling are probably the unusually steep flanks of the domes in the supra-salt for mation, development of inverse folding in the evaporite-underlying layers, and a general history of the basin deformations. The flanks of the domes and, especially, the overhangs formed by the top of evaporites can be related to small (but easily accessible) deposit areas in the upper, supra-salt part of the basin; the study of inverse folding beneath evaporites is of extreme interest in the context of the search for giant fields. The exploration in subsalt layers is related to expensive deep drilling, so that preliminary and accompanying geological-geophysical studies have to be especially thorough and involve all the methods available. In particular, because of the lack of direct information on the subsalt objects, use can be made of the subsalt structure prediction based on geodynamic modeling whose results can be refined by testing the method on the detailed-drilling site.

6. CONTRIBUTION OF THE AUTHORS

All authors made an equivalent contribution to this article, read and approved the final manuscript.

7. DISCLOSURE

The authors declare that they have no conflicts of interest relevant to this manuscript.

8. REFERENCES

Abramov T., Lavrentiev M., Lunev B., 2016. Implementation and Testing of the Fast Numerical Algorithm for Simulation of 3D Gravity Creeping Flow of Incompressible Newtonian Fluid. In: E. Pyshkin, V. Klyuev, A. Vazhenin (Eds), ICAIT-2016. Proceedings of the 2nd International Conference on Applications in Information Technology (October 6–8, 2016). The University of Aizu Press, Aizu-Wakamatsu, Japan, p. 121–124.

Abramov T.V., 2015. Massively Parallel Calculation of the Rayleigh-Taylor Instability Using the Analytical Expression of the Green's Function of the Corresponding Boundary Value Problem. Computational Technologies 20 (4), 3–16 (in Russian) [Абрамов Т.В. Массивно-параллельный расчет неустойчивости Релея-Тейлора с помощью аналитического выражения функции Грина соответствующей краевой задачи // Вычислительные технологии. 2015. Т. 20. № 4. С. 3–16].

Abramov T.V., Lunev B.V., 2014. Modeling of Salt Diapirism by Calculation of Three-Dimensional Creeping Currents Using CUDA® Parallel Computing Technology on GPU. CUDA Almanac, 10 p. (in Russian) [Абрамов Т.В., Лунёв Б.В. Моделирование соляного диапиризма расчетом трехмерных ползущих течений с использованием технологии параллельных вычислений CUDA® на GPU // CUDA альманах. 2014. 10 с.].

Abramov T.V., Lunev B.V., Lapkovsky V.V., 2018. A Software System for Modeling Evolution in a Sedimentary Basin Complicated by the Processes of Salt Tectogenesis Due to the Content of Salt-Bearing Rocks. Software Registration Certificate № RU 2018612365 of November 09, 2021. ROSPATENT (in Russian) [Абрамов Т.В., Лунев Б.В., Лапковский В.В. Программа для моделирования эволюции осадочного бассейна, осложненной процессами соляного тектогенеза из-за содержания соленосных пород: Свидетельство о государственной регистрации программы для ЭВМ № RU 2018612365 от 16.02.2018 г. РОСПАТЕНТ, 2018].

Antipov M.P., Volozh Yu.A., 2012. Features of the Structure and Oil and Gas Content of the Post-Salt Section of the Precaspian Depression. Oil and Gas 1 (67), 47–71 (in Russian) [Антипов М.П., Волож Ю.А. Особенности строения и нефтегазоносность надсолевого разреза прикаспийской впадины // Нефть и газ. 2012. № 1 (67). С. 47–71].

Bakirov K.Kh., Kurmanov S.K., Chimbulatov M.A., Korkeev V.I., Ogai B.A., Chanyshev P.Kh., Khabibullin E.G., 1992. Vertical Migration of Hydrocarbons and the Forecast of Large Prospects for the Industrial Oil and Gas Potential of the Permian-Triassic Complex of Deposits of the Precaspian Depression. Alma-Ata – Aktyubinsk, 215 p. (in Russian) [Бакиров К.Х., Курманов С.К., Чимбулатов М.А., Коркеев В.И., Огай Б.А., Чанышев Р.Х., Хабибуллин Э.Г. Вертикальная миграция углеводородов и прогноз крупных перспектив промышленной нефтегазоносности пермотриасового

комплекса отложений Прикаспийской впадины // Алма-Ата – Актюбинск, 1992. 215 с.].

Eskozha B.A., Voronov G.V., Kuantaev N.E., Trokhimenko M.S., Shudabaev M.S., Madzhanov K.K., 2007. The Post-Salt Complex in the South of the Caspian Basin Is Still Promising for Oil and Gas Discovery. News of National Academy of Sciences of the Republic of Kazakhstan. Series of Geology and Technical Sciences 6, 33–49 (in Russian) [Ескожа Б.А., Воронов Г.В., Куантаев Н.Е., Трохименко М.С., Шудабаев М.С., Маджанов К.К. Надсолевой комплекс юга Прикаспийской впадины по-прежнему перспективен для обнаружения нефти и газа // Известия НАН РК. Серия геологии и технических наук. 2007. № 6. С. 33–49].

Filippov Yu.F., Lapkovskii V.V., Lunev B.V., 2009. Numerical Modeling of Salt Tectogenesis in the Cambrian Deposits of the Cis-Yenisei Sedimentary Basin (PR3-Pz) (West Siberia). Russian Geology and Geophysics 50 (2), 96–103. https://doi.org/10.1016/j.rgg.2008.08.001.

Jackson M.P.A., Talbot C.J., 1986. External Shapes, Strain Rates and Dynamics of Salt Structures. Geological Society of America Bulletin 97, 305–323. https://doi.org/10.1130/0016-7606(1986)97<305:ESSRAD>2.0.CO;2.

Konishchev V.S., 1982. Tectonics of Halokinesis Regions of the East European and Siberian Platforms. Publishing House of Science and Technology, Minsk, 258 p. (in Russian) [Конищев В.С. Тектоника областей галокинеза Восточно-Европейской и Сибирской платформ. Минск: Наука и техника, 1982. 258 с.].

Konishchev V.S., Volozh Yu.A., Nurbaev B.O., 1990. Halokinesis in Secondary Saline Strata. Doklady of the Academy of Sciences of BSSR 34 (8), 736–739 (in Russian) [Конищев В.С., Волож Ю.А., Нурбаев Б.О. Галокинез во вторичных соленосных толщах // Доклады АН БССР. 1990. Т. 34. № 8. С. 736–739].

Kontorovich V.A., Lunev B.V., Lapkovsky V.V., 2019. Geological and Geophysical Characteristics of the Anabar-Khatanga Oil and Gas Region; Numerical Modeling of Salt Dome Formation Processes (Siberian Sector of the Russian Arctic). Geodynamics & Tectonophysics 10 (2), 459–470 (in Russian) [Конторович В.А., Лунев Б.В., Лапковский В.В. Геолого-геофизическая характеристика Анабаро-Хатангской нефтегазоносной области; численное моделирование процессов формирования соляных куполов (Сибирский сектор Российской Арктики) // Геодинамика и тектонофизика. 2019. Т. 10. № 2. С. 459–470]. https://doi.org/10.5800/GT-2019-10-2-0421.

Kontorovich V.A., Lunev B.V., Lapkovsky V.V., Filippov Yu.F., 2014. Numerical Models of the Formation of Salt Tectonics Structures Identified by Seismic Exploration in the Cambrian Deposits of the Cis-Yenisei Sedimentary Basin (Southeast of Western Siberia). Geology and Mineral Resources of Siberia 2, 105–115 (in Russian) [Конторович В.А., Лунёв Б.В., Лапковский В.В., Филиппов Ю.Ф. Численные модели формирования структур соляной тектоники, выявленных сейсморазведкой в кембрийских отложениях Предъенисейского осадочного бассейна (юго-восток Западной Сибири) // Геология и минерально-сырьевые ресурсы Сибири. 2014. № 2. С. 105–115].

Kosygin Yu.A., 1950. Salt Tectonics of Platform Areas. Gostoptekhizdat, Moscow, 248 p. (in Russian) [Косыгин Ю.А. Соляная тектоника платформенных областей. М.: Гостоптехиздат, 1950. 248 с.].

Kosygin Yu.A., 1960. Types of Salt Structures in Platform and Geosynclinal Areas. Publishing House of the USSR Academy of Science, Moscow, 91 p. (in Russian) [Косыгин Ю.А. Типы соляных структур платформенных и геосинклинальных областей. М.: Изд-во АН СССР. 1960. 91 с.].

Kuandykov B.M., Matloshinsky N.G., Sentgiorgi K., Kovach A., Trokhimenko M.S., Eskozha B., Milota K., Fogarashi A., Li Yanchen, Gonts G., Turkov O.S., Nazarov M.Sh., 2011. Oil and Gas Content of the Paleozoic Shelf Margin of the North of the Precaspian Depression. Gylym Publishing House, Almaty, 280 p. (in Russian) [Куандыков Б.М., Матлошинский Н.Г., Сентгиорги К., Ковач А., Трохименко М.С., Ескожа Б., Милота К., Фогараши А., Ли Янчен, Гонц Г., Турков О.С., Назаров М.Ш. Нефтегазоность палеозойской шельфовой окраины севера Прикаспийской впадины. Алматы: Изд-во Гылым, 2011. 280 с.].

Lunev B.V., Abramov T.V., Lapkovsky V.V., Priymenko V.I., 2017a. An Efficient 3D Modeling of Salt Tectogenesis for Prediction Subsalt Structure. Technologies of Seismic Prospecting 3, 96–103 (in Russian) [Лунев Б.В., Абрамов Т.В., Лапковский В.В., Прийменко В.И. Высокоэффективное 3D моделирование соляного тектогенеза в целях прогноза структуры подсолевого комплекса // Технологии сейсморазведки. 2017. № 3. С. 96–103].

Lunev B.V., Lapkovsky V.V., 2009. Rapid Numerical Modeling of Salt Tectonics: Possibility of Operational Use in Geological Practice. Physical Mesomechanics 12 (1), 63–74 (in Russian) [Лунёв Б.В., Лапковский В.В. Быстрое численное моделирование соляной тектоники: возможность оперативного использования в геологической практике // Физическая мезомеханика. 2009. Т. 12. №1. С. 63–74].

Lunev B.V., Lapkovsky V.V., 2014. Mechanism of Development of Inversion Folding in the Subsalt. Izvestiya, Physics of the Solid Earth 50, 57–63. https://doi.org/10.1134/S1069351314010066.

Lunev B.V., Lapkovsky V.V., Kanakov M.S., Zastrozhnov A.S., 2017b. Solution of the Evolutionary Inverse Problem to Refine the Geological Structure in the Areas of Salt Tectonics. In: Marchuk Scientific Readings – 2017. Proceedings of the International Science Conference (June 25 – July 14, 2017). ICMMG SB RAS, Novosibirsk, p. 556–662 (in Russian) [Лунев Б.В., Лапковский В.В., Канаков М.С., Застрожнов А.С. Решение эволюционной обратной задачи для уточнения геологической структуры в областях соляной тектоники // Марчуковские научные чтения – 2017: Труды Международной научной конференции (25 июня – 14 июля 2017 г.). Новосибирск: ИВМиМГ СО РАН, 2017. С. 557–563].

Matusevich A.V., 2005. Gravimetric Modeling of Salt-Bearing Deposits in the Precaspian Basin. The Top of Salt Regional Model. News of National Academy of Sciences of the Republic of Kazakhstan. Series of Geology and Technical Sciences 6, 33–56 (in Russian) [Матусевич А.В. Гравиметрическое моделирование соленосных отложений

Прикаспийской впадины. Региональная модель кровли соли // Известия НАН РК. Серия геологии и технических наук. 2005. № 6. С. 33–56].

Matusevich A.V., 2007. Zoning of the Salt Domes of the Pre-Caspian Depression Taking into Account the Structure of the Gravitational Field. News of National Academy of Sciences of the Republic of Kazakhstan. Series of Geology and Technical Sciences 2, 26–44 (in Russian) [Матусевич А.В. Районирование соляных куполов Прикаспийской впадины с учетом структуры гравитационного поля // Известия НАН РК. Серия геологии и технических наук. 2007. № 2. С. 26–44].

Pisarenko Yu.A., Goncharenko O.P., Pisarenko V. Yu., 2021a. Structural Features of the Lower Permian Salt-Bearing Series and the Character of Salt-Tectogenesis Manifestations in the Northern and Northwestern Margins of the Caspian Depression. Paper I. Izvestiya of Saratov University. Earth Sciences 21 (1), 58–64 (in Russian) [Писаренко Ю.А., Гончаренко О.П., Писаренко В.Ю. Особенности строения нижнепермской соленосной толщи и характер проявления соляного тектогенеза в северном и северо-западном обрамлении Прикаспийской впадины. Статья 1 // Известия Саратовского университета. Новая серия. Серия Науки о Земле. 2021. Т. 21. № 1. С. 58–64]. https://doi.org/10.18500/1819-7663-2021-21-1-58-64.

Pisarenko Yu.A., Goncharenko O.P., Pisarenko V.Yu., 2021b. Structural Features of the Lower Permian Salt-Bearing Series and the Character of Salt-Tectogenesis Manifestations in the Caspian Depression. Paper II. Izvestiya of Saratov University. Earth Sciences 21 (2), 93–102 (in Russian) [Писаренко Ю.А., Гончаренко О.П., Писаренко В.Ю. Особенности строения нижнепермской соленосной толщи и характер проявления соляного тектогенеза в северном и северо-западном обрамлении Прикаспийской впадины. Статья II // Известия Саратовского университета. Новая серия. Серия Науки о Земле. 2021. Т. 21. № 2. С. 93–102]. https://doi.org/10.18500/1819-7663-2021-21-2-93-102.

Pisarenko Yu.A., Pisarenko V.Yu., Dunaeva M.N., 2017. Stratigraphical, Lithological-Facies and Structural Relationships of Salt-Bearing Rocks of Different Ages and Their Role in the Manifestation of Processes of Salt Tectogenesis, Forecasting the Structure of the Subsalt Bed within the Sol-Iletsk Dome. Interior of Povolzhye and Pricaspian Region 90, 3–10 (in Russian) [Писаренко Ю.А., Писаренко В.Ю., Дунаева М.Н. Стратиграфические, литолого-фациальные и структурные соотношения разновозрастных соленосных пород и их роль в проявлении процессов соляного тектогенеза, прогнозе структуры подсолевого ложа в пределах Соль-Илецкого свода // Недра Поволжья и Прикаспия. 2017. Вып. 90. С. 3–10].

Pisarenko Yu.A., Pisarenko V.Yu., Kireenko O.S., Goncharenko O.P., 2011. Model of Permian Stage of Salt Accumulation of South-Eastern Part of Russian Plate and Its Significance for Exploring Fields of Oil and Gas and Different Types of Mineral Resources. Geology and Oil and Gas 1, 44–52 (in Russian) [Писаренко Ю.А. Писаренко В.Ю., Киреенко О.С., Гончаренко О.П. Модель пермского этапа соленакопления юго-восточной части Русской плиты и ее значение для поиска месторождений нефти и газа и различных видов полезных ископаемых // Геология и нефти и газа. 2011. № 1. С. 44–52].

Poliakov A.N.B., van Balen R., Podladchikov Yu., Daudre B., Cloetingh S., Talbot C., 1993. Numerical Analysis of How Sedimentation and Redistribution of Surficial Sediments Affects Salt Diapirism. Tectonophysics 226 (1–4), 199–216. https://doi.org/10.1016/0040-1951(93)90118-4.

Ramberg H., 1985. Gravity and Deformation in the Earth's Crust. Nedra, Moscow, 399 p. (in Russian) [Рамберг Х. Сила тяжести и деформации в земной коре. М.: Недра, 1985, 399 с.].

Tikhvinsky I.N., 1974. Stratigraphy and Potassium-Bearing Horizons of the Kungur of the Precaspian Syneclise. Soviet Geology 5, 44–54 (in Russian) [Тихвинский И.Н. Стратиграфия и калиеносные горизонты кунгура Прикаспийской синеклизы // Советская геология. 1974. № 5. С. 44–54].

Volozh Yu.A., 1971. Methodology for Studying the Regional Structure of the Precaspian Basin in Order to Identify Zones of Oil and Gas Potential (Based on the Volumetric Method of Power Analysis). Brief PhD Thesis (Candidate of Geology and Mineralogy). Moscow, 25 p. (in Russian) [Волож Ю.А. Методика изучения региональной структуры Прикаспийской впадины с целью выделения зон нефтегазоносности (на основе объемного метода анализа мощностей): Автореф. дис. ... канд. геол.-мин. наук. М., 1971. 25 с.].

Volozh Yu.A., Konishchev V.S., 1989. Tectonic Zonality of Salt Structures in Areas of Halokinesis. Doklady of the Academy of Sciences of BSSR 33 (9), 832–836 (in Russian) [Волож Ю.А., Конищев В.С. Тектоническая зональность соляных структур областей галокинеза // Доклады АН БССР. 1989. Т. 33. № 9. С. 832–836].

Volozh Yu.A., Lipatova V.V., Bukina T.F., Yanochkina Z.A., 2000. Features of the Structure of the Upper Permian Deposits of the South and Southeast of the Precaspian Depression. Interior of Povolzhye and Pricaspian Region 22, 10–22 (in Russian) [Волож Ю.А., Липатова В.В., Букина Т.Ф., Яночкина З.А. Особенности строения верхнепермских отложений юга и юго-востока Прикаспийской впадины // Недра Поволжья и Прикаспия. 2000. Вып. 22. С. 10–22].

Volozh Yu.A., Miletenko N.V., Kuantaev N.E., Lipatova V.V., 1997a. Prospects for the Development of Oil and Gas Prospecting in the Post-salt Complex of the Precaspian Depression. Interior of Povolzhye and Pricaspian Region 14, 7–11 (in Russian) [Волож Ю.А., Милетенко Н.В., Куантаев Н.Е., Липатова В.В. Перспективы развития нефтегазопоисковых работ в надсолевом комплексе Прикаспийской впадины // Недра Поволжья и Прикаспия. 1997. Вып. 14. С. 7–11].

Volozh Yu.A., Parasyna V.S. (Eds), 2008. Astrakhan Carbonate Massif: Structure and Oil and Gas Potential. Nauchnyi Mir, Moscow, 221 p. (in Russian) [Астраханский карбонатный массив: Строение и нефтегазоносность // Ред. Ю.А. Волож, В.С. Парасына. М.: Научный мир, 2008. 221 с.].

Volozh Yu.A., Talbot C.J., Ismail-Zadeh A.T., 2003. Salt Structures and Hydrocarbons in the Pricaspian Basin. AAPG Bulletin 87 (2), 313–334. DOI:10.1306/09060200896.

Volozh Yu.A., Volchegursky L.F., Groshev V.G., Shishkina T.Yu., 1997b. Types of Salt Structures in the Precaspian Depression. Geotectonics 31 (3), 204–217.

Volozh Yu.A., Votsalevsky E.S., Zhivoderov A.B., Nurbaev B.O., Pilifosov V.M., 1989. Problems of Oil and Gas Potential of Post-Salt Deposits of the Pre-Caspian Depression. Bulletin of the Kazakh SSR Academy of Sciences. Geological Series 4, 3–15 (in Russian) [Волож Ю.А., Воцалевский Э.С., Живодеров А.Б., Нурбаев Б.О., Пилифосов В.М. Проблемы нефтегазоносности надсолевых отложений Прикаспийской впадины // Известия АН КазССР. Серия геологическая. 1989. № 4. С. 3–15].

Yatskevich S.V., Markina N.N., Taskinbaev K.M., Alzhanov A.A., 1990. Stratigraphic Section in the Superimposed Trough of the Karakuduk Dome. Geology of Oil and Gas 7, 36–39 (in Russian) [Яцкевич С.В., Маркина Н.Н., Таскинбаев К.М., Альжанов А.А. Стратиграфический разрез в наложенной мульде купола Каракудук // Геология нефти и газа. 1990. № 7. С. 36–39].

Zholtaev G.Zh., 1966. Morphological Types of Salt Accumulation in the Eastern Part of the Caspian Depression. Oil and Gas Geology and Geophysics 2, 15–21 (in Russian) [Жолтаев Г.Ж. Морфологические типы скопления соли в восточной части Прикаспийской впадины // Нефтегазовая геология и геофизика. 1966. № 2. С. 15–21].

Zhuravlev V.S., 1963. Types of Salt Domes in the Precaspian Depression. In: N.P. Kheraskov (Ed.), Problems of Regional Tectonics of Eurasia. Publishing House of the USSR Academy of Science, Moscow, p. 162–201 (in Russian) [Журавлев В.С. Типы соляных куполов Прикаспийской впадины // Проблемы региональной тектоники Евразии / Ред. Н.П. Херасков. М.: Изд-во АН СССР, 1963. С. 162–201].

Zhuravlev V.S., 1964. Comparative Tectonics of the Pechora, Precaspian and North Sea Exogonal Depressions of the European Platform. Proceedings of the Geological Institute of the USSR Academy of Science. Iss. 232. Nedra, Moscow, 397 p. (in Russian) [Журавлев В.С. Сравнительная тектоника Печорской, Прикаспийской и Североморской экзогональных впадин Европейской платформы // Труды ГИН АН СССР. М.: Недра, 1964. Вып. 232. 397 с.].

Zhuravlev V.S., 1966. Classification of Local Structures of the Precaspian Depression. In: Materials on Geology and Minerals of the Western Kazakhstan. Nauka, Alma-Ata, p. 110–116. (in Russian) [Журавлев В.С. Классификация локальных структур Прикаспийской впадины // Материалы по геологии и полезным ископаемым Западного Казахстана. Алма-Ата: Наука, 1966. С. 110–116].